

## A Multi-continuum Method for Studying the Effect of Inactive Fractures on Solute Transport in 2-D Discrete Fracture Network

Zhen Wang<sup>1</sup>, Jonny Rutqvist<sup>2</sup>, Ying Dai<sup>1</sup>

**Abstract:** Fractures in a discrete fracture network can be divided into two parts: Active fractures, which form a connected fracture network and dominate fluid flow and solute transport; and inactive fractures, which are dead-end parts of the fractures (isolated fractures will be incorporated into rock matrix) and do not contribute significantly to the fluid flow, but maybe important for the solute transport, especially for rock matrix diffusion. We present a multi-continuum method (including active fracture continuum, inactive fracture continuum and matrix continuum), which is based on the “multiple interacting continua” method, to describe fluid flow and solute transport in fractured media, including interactions of (1) active fractures with inactive fractures, (2) active fractures with matrix and (3) inactive fractures with matrix. A 2-D discrete fracture network is transformed into a coarse-scale grid-based equivalent continuum model, and each coarse-scale block is discretized into overlying sub-blocks including active fracture continuum, inactive fracture continuum and nested matrix continua with equivalent properties based on local fracture geometry information. The permeability tensor for the sub-block associated with active fracture continuum is determined from local flow simulations using the underlying discrete fracture network. The permeability for inactive fracture continuum and matrix continuum is assigned with very small value as they do not significantly contribute to the fluid flow. With this upscaling method, we established a heterogeneous, anisotropic permeability tensor field in the study domain. The above methodology was applied to a 2D BMT (benchmark test) of the international cooperative project DECOVALEX 2011. This benchmark test consists of a  $20 \times 20$  m model domain including a 2-D fracture-network of 7797 individual fractures with apertures of each fracture correlated to their length. The simulation results show that the inactive fractures will enhance rock matrix diffusion, which is

<sup>1</sup> School of Aerospace Engineering and Applied Mechanics, Tongji University, Shanghai 200092, China.

<sup>2</sup> Earth Science Division, Lawrence Berkeley National Laboratory (LBNL), Berkeley, CA 94720 USA.

consistent with observations at field experiments as reported in the literatures, and thus play an important role in solute transport in fractured media.

**Keywords:** Multi-continuum model, MINC method, Inactive fractures, 2-D discrete fracture network, solute transport

## 1 Introduction

Fractured media may be represented by stochastic discrete fracture network-matrix system [Min, Jing and Stephansson (2004); Zuo, Peng, Li, Chen and Xie (2009)]. In such a system, global flow is assumed to occur only through the network of interconnected fractures, whereas fractures and rock matrix can exchange mass and heat locally. With a detailed fracture characterization, fluid flow and solute transport in fractured media can be investigated using a discrete fracture network (DFN) model directly [Baghbanan and Jing (2007); Gato and Shie (2008); Zuo, Xie, Zhou and Peng (2010); Zhao, Jing, Neretnieks and Moreno (2011); Smith, Crocker, Flewitt and Mahalingam (2012);] or using an equivalent continuum model with upscaled hydrological parameters from the underlying discrete fracture network [Long, Remer, Wilson, and Witherspoon (1982); Oda (1985); Dershowitz, Lapointe, Eiben and Wei (2000); Rutqvist, Leung, Hoch, Wang and Wang (2013)], and the interaction of fractures with matrix can hence be captured through characterizing fractures and matrix explicitly with different hydrologic parameters [Doughty, Salve and Wang (2002); An, Wu, and Gao (2012)], or through a dual-continuum strategy with a transfer function linking fracture with matrix [Barenblatt, Zheltov and Kochina (1960); Warren and Root (1963); Dogan, Class and Helmig (2009)], or through an “multiple interacting continua” method which treats the fracture-matrix interaction in a fully transient way by a subgridding technique [Pruess and Narasimhan (1982) Karimi-Fard, Gong and Durlinsky (2006); Tatomir, Szymkiewicz, Class and Helmig (2011)]. However, not all the fractures have the same impact on flow and transport. The dead-end parts of fractures and isolated fractures do usually not contribute significantly to the fluid flow, but may still be important for solute transport, because they will increase contact areas between fractures and matrix, which may potentially impact overall flow and transport behavior.

To investigate the effect of dead-end parts of fractures on solute transport, we conceptualize the original fracture-matrix system as three parts: (1) active fractures, which are connected globally and dominate the fluid flow and solute transport; (2) inactive fractures, which are dead-end parts of fractures and has little contribution to fluid flow; (3) matrix, including isolated fractures which here are considered as part of the matrix. The importance of inactive fractures on transport was also shown by Zhou, Liu, Bodvarsson and Molz (2006) and Zhou, Liu, Molz, Zhang

and Bodvarsson (2007) from literature survey of field scale experiments. They considered diffusion into stagnant water and infilling material within fractures as one of the reasons of the observed enhancement of field-scale matrix diffusion. Neretnieks (2002) used a stochastic multi-channel model, which could model diffusion into stagnant water regions, to analyze tracer tests in fractured rock. Wu, Liu and Bodvarsson (2004) used a triple-continuum model to investigate the effect of “small fractures” (a similar definition of inactive fractures) on flow and transport in the unsaturated zone at Yucca Mountain (Nevada) and calibrate its hydrological parameters to field-scale tests.

In this paper, we present an alternative way of treating inactive fractures by using a multi-continuum approach, which is based on the “multiple interacting continua (MINC)” method considering fully transient inter-porosity flow [Pruess and Narasimhan (1982); Pruess, Oldenburg and Moridis (1999)]. Using this approach, we study the effect of inactive fractures on solute transport in a 2D discrete fracture network, with the effective hydrological parameters upscaled from the underlying discrete fracture network and matrix. A detailed explanation for the multi-continuum approach is given in Section 2. Then, in Section 3, we first present a comparison of our multi-continuum model with an analytical solution of triple porosity model, and thereafter apply the multi-continuum approach to a 2D DFN benchmark test, that was part of the international cooperative project DECOVALEX 2011.

## **2 Multi-continuum Model**

### ***2.1 Comparison with other conceptual models for handling fracture-matrix interaction***

Figure 1 illustrates the multi-continuum concept compared to MINC, and triple-continuum concept [Wu, Liu and Bodvarsson (2004)]. These three modeling concepts are focused on the handling of fracture-matrix interaction. The MINC method [Pruess and Narasimhan (1982)] adopts the classical double-porosity approach [Warren and Root (1963)] involving a continuum treatment for both the fracture network and the porous rock matrix (Fig.1 (b)). The double-porosity method assumes that the inter-porosity flow is “quasi-steady”, while the MINC method considers fully transient inter-porosity flow by sub-gridding of the matrix domain into sequence of nested computational volume elements (Fig.1 (b)), which is based on the assumption that the thermodynamic properties of the matrix vary with the distance from the nearest fracture. Consequently, the crucial point of the MINC method is the partitioning (or discretization) procedure adopted for inter-porosity flow. More details about MINC method can be found in Pruess and Karasaki (1982); Pruess

(1983) and Pruess and Narasimhan (1982).

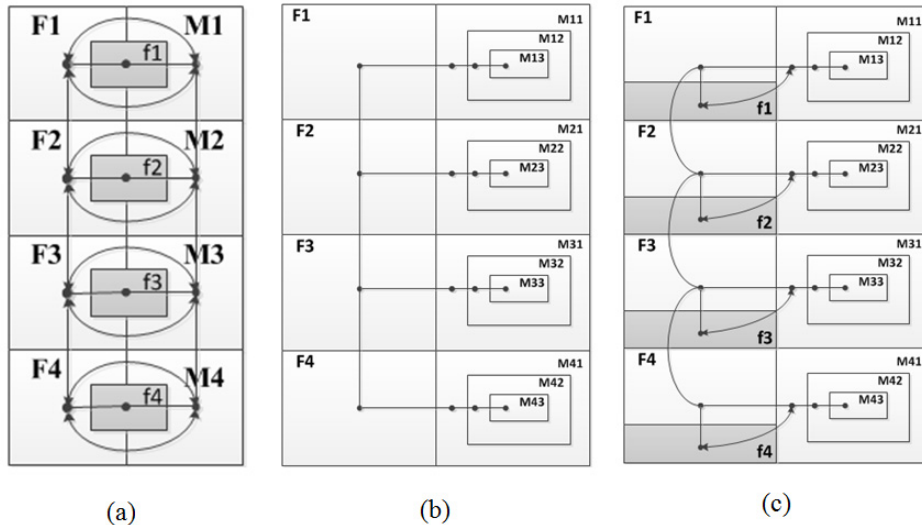


Figure 1: Schematic of different conceptualizations for partitioning a fracture-matrix system: (a) Triple-continuum model; (b) MINC model; (c) Multi-continuum model. (M=matrix; F=Active fractures; f=inactive fractures) Modified from [Doughty (1999) and Wu, Liu and Bodvarsson (2004)]

The multi-continuum method involving inactive fractures extends the MINC concept by adding one more connection (via inactive-fracture continuum) between active-fracture continuum and matrix continuum (Fig.1 (c)), which is like the idea of the triple-continuum concept. However, differences exist between multi- and triple-continuum models. The triple-continuum is an extension of the double-permeability model, which can consider matrix-matrix flow, but still assume a quasi-steady fracture-matrix flow; while the multi-continuum model enables transient matrix responses. Besides, the triple-continuum model uses two sets of fracture geometric parameters such as fracture spacing for active and inactive fractures respectively; while the multi-continuum model considers active and inactive fractures as one pattern of fractures, and therefore uses only one fracture spacing. Thus, the multi-continuum model partitions the fracture-matrix system into three kinds of continua: active-fracture continuum, inactive-fracture continuum and nested matrix continua. And can handle active fracture-matrix (F-M) interaction, inactive fracture-matrix (f-M) interaction, and active fracture-inactive fracture (F-f) interaction.

Principally, the multi-continuum model still follows the assumptions of the MINC model [Pruess (1983)] as:

- (1) Approximate thermodynamic equilibrium exists locally within each of the three continua at all times at a given location.
- (2) The fracture network is sufficiently well connected throughout the considered fractured porous domain.
- (3) The thermodynamic conditions in the rock matrix are considered to depend only on the distance from the nearest fracture.

## 2.2 Numerical implementation

The numerical implementation of the multi-continuum discussed above is based on the framework of integral finite difference method in the TOUGH2 multiphase flow and heat transport simulator [Pruess, Oldenburg and Moridis (1999)]. The multi-continuum method uses the similar partitioning scheme as the MINC method. For a 2-D discrete fracture network (Fig.2 (a)), the “primary mesh” (Fig.2 (b)) is first specified in terms of integral finite difference form by means of a set of coarse blocks with volume  $V_n$  ( $n= 1, 2, \dots, N$ ), interface areas  $A_{nm}$ , and nodal distance  $D_{nm}$ . Second, the “secondary mesh” (the complete computational mesh) is generated by sub-gridding each grid block of the primary mesh into a sequence of overlapping interacting sub-continua, including active-fracture continuum, inactive-fracture continuum and a series of matrix continua (see Fig.2 (c)). All inter-block connections ( $A_{nm}, D_{nm}$ ) and permeability of the primary mesh are assigned to the active-fracture system in which global flow and transport occurs. Additional intra-block connections are generated to permit mass exchange between sub-continua. Fig. 2 (d) describes the representative intra-block connections of F-M, f-M, F-f and M-M.

### 2.2.1 Determination of intra-block connections

In one element of the secondary mesh (Fig.2 (d)), assume that the active and inactive fracture volume fractions are known as  $\phi_F$  and  $\phi_f$ , respectively, with the fracture spacing  $FS$  of the original fracture system composed of both active and inactive fractures. With the original fracture volume fraction ( $\phi_{\mathbb{F}} = \phi_F + \phi_f$ , where subscript  $\mathbb{F}$  denotes original fractures,  $F$  and  $f$  for active and inactive fractures respectively in this context), fracture spacing  $FS$  and the “proximity function” in the MINC method we can determine the interface area  $A_{\mathbb{F}-M}$ ,  $A_{M-M}$  and nodal distance  $D_{\mathbb{F}-M}$ ,  $D_{M-M}$  (Pruess 1983). Then the interface area, nodal distance of F-M, f-M and F-f, and volume of each sub-continuum can be obtained through the aforementioned parameters, and are listed in Tab. 1. The volumes of active- and inactive-fracture continua ( $V_F$  and  $V_f$ ) are calculated by their fracture volume

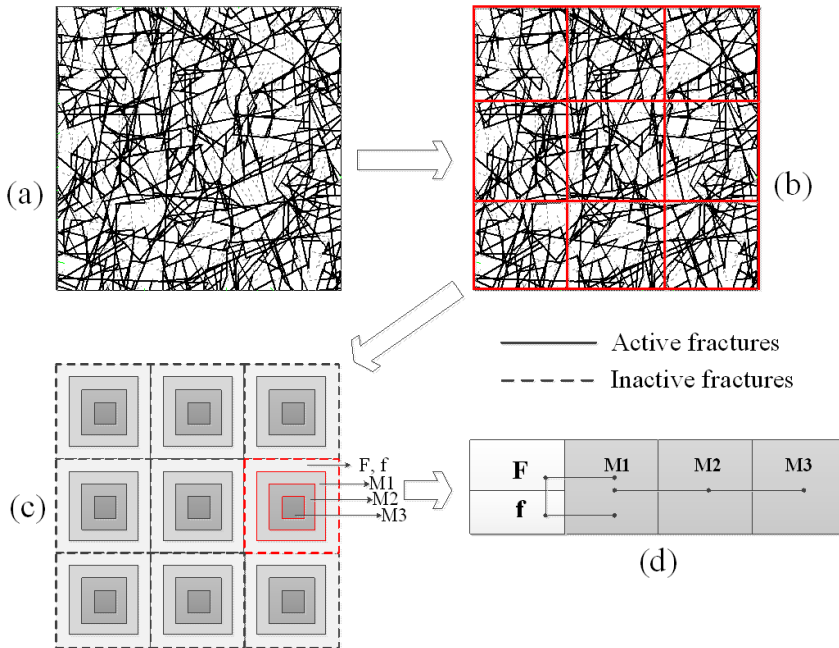


Figure 2: Schematic of mesh construction of multi-continuum model. (a) Original discrete fracture network including active and inactive fractures; (b) Primary mesh of fracture-matrix system; (c) Secondary mesh of fracture-matrix system; (d) A representative element of secondary mesh.

fraction and coarse block volume ( $V_n$ ). Each matrix continuum volume ( $V_M$ ) is obtained by dividing the total matrix volume by the number of matrix continua. Interface area of F-M and f-M ( $A_{F-M}$ ,  $A_{f-M}$ ) are proportional to their relative fracture volume fraction. Nodal distance of F-M and f-M ( $D_{F-M}$ ,  $D_{f-M}$ ) are same as  $D_{F-M}$  based on the notion that the active and inactive fractures belong to the same pattern of fractures. Interface area ( $A_{F-f}$ ) and nodal distance ( $D_{F-f}$ ) between active and inactive fracture continua are treated using geometry of inactive fractures with the introduction of a characteristic length ( $l_f$ ) of inactive fractures.

### 2.2.2 Determination of model parameters in a 2-D DFN

In a 2-D DFN system with a unit thickness, the model parameters for each coarse block can be determined by geometric information of fractures in that block. The

Table 1: Geometric parameters of intra-block connections

Interacting Type	Sub-continuum Volume	Interface Area	Nodal Distance
F-M	$V_F = \phi_F V_n$	$A_{F-M} = \phi_F A_{\mathbb{F}-M}$	$D_{F-M} = D_{\mathbb{F}-M}$
f-M	$V_f = \phi_f V_n$	$A_{f-M} = (1 - \phi_F) A_{\mathbb{F}-M}$	$D_{f-M} = D_{\mathbb{F}-M}$
F-f		$A_{F-f} = V_f / l_f$	$D_{F-f} = l_f / 2$
M-M	$V_M = (1 - \phi_{\mathbb{F}}) V_n / N_M$	$A_{M-M}$	$D_{M-M}$

Note in Tab. 1,  $\phi_F = \phi_F / (\phi_F + \phi_f)$  is the relative active fracture volume fraction;  $N_M$  is number of matrix continua.

active and inactive fracture volume fraction is:

$$\varphi_F = \sum_{i=1}^{N_F} \frac{l_{Fi} a_{Fi}}{A_n}, \tag{1}$$

$$\varphi_f = \varphi_{\mathbb{F}} - \varphi_F, \tag{2}$$

where  $\varphi_{\mathbb{F}} = \sum_{i=1}^{N_{\mathbb{F}}} \frac{l_{\mathbb{F}i} a_{\mathbb{F}i}}{A_n}$  is the original fracture volume fraction,  $N_{\mathbb{F}}$  and  $N_F$  is the number of original fractures and active fractures in the coarse block respectively,  $A_n$  is the area of the block,  $l_{\mathbb{F}i}$  and  $l_{Fi}$  is the length of an original fracture and an active fracture,  $a_{\mathbb{F}i}$  and  $a_{Fi}$  is the aperture of an original fracture and an active fracture.

To determine the characteristic length of inactive fractures ( $l_f$ ), we assume that each original fracture has a part that could be classified as an inactive fracture, and then  $l_f$  can be obtained by

$$l_f = \frac{\varphi_f A_n}{\sum_{i=1}^{N_{\mathbb{F}}} a_{\mathbb{F}i}}. \tag{3}$$

The proximity function in the MINC method for an idealized 1-D fracture set and 2-D two perpendicular fracture sets (as shown in Fig.3, the matrix blocks are partitioned uniformly by fractures.) is  $\text{PROX}(x) = \frac{2}{a}x$  and  $\text{PROX}(x) = \frac{2(a+b)}{ab}x - \frac{4}{ab}x^2 = (\frac{2}{a} + \frac{2}{b})x - \frac{4}{ab}x^2$  respectively [Pruess (1983)]. Where  $a$  and  $b$  is fracture spacing in respective horizontal and vertical directions, and  $x$  is the distance from a fracture. The first term of the proximity function  $\frac{2}{a}$  or  $\frac{2(a+b)}{ab}$  is just equal to the fracture areal intensity parameter  $P_{32}$  in one block (Fig.3), where  $P_{32}$  can be estimated in two-dimensional cases, the average fracture length per unit area [Xu, Dowd, Mardia, and Fowell (2006)]. Consequently, we can estimate fracture spacing from  $P_{32}$  by equating random fractures in the block to an idealized fracture pattern (Fig. 3)

based on the fracture distribution. The fracture spacing for fractures which can be equated to a 1-D fracture set is

$$FS = \frac{2}{P_{32}} = 2 / \frac{\sum_{i=1}^{N_F} l_{Fi}}{A_n}. \tag{4}$$

Whereas the fracture spacing for fractures which can be equated to a 2-D fracture set is

$$FS_h = \frac{2}{P_{32v}} = 2 / \frac{\sum_{i=1}^{N_{FV}} l_{Fi}}{A_n}, \tag{5}$$

$$FS_v = \frac{2}{P_{32h}} = 2 / \frac{\sum_{i=1}^{N_{FH}} l_{Fi}}{A_n}, \tag{6}$$

where  $FS_h$  and  $FS_v$  is the fracture spacing in horizontal and vertical direction respectively,  $P_{32v}$  and  $P_{32h}$  is the fracture areal intensity parameter in vertical and horizontal direction respectively, and  $N_{FV}$  and  $N_{FH}$  is the number of fractures in vertical and horizontal direction, respectively.

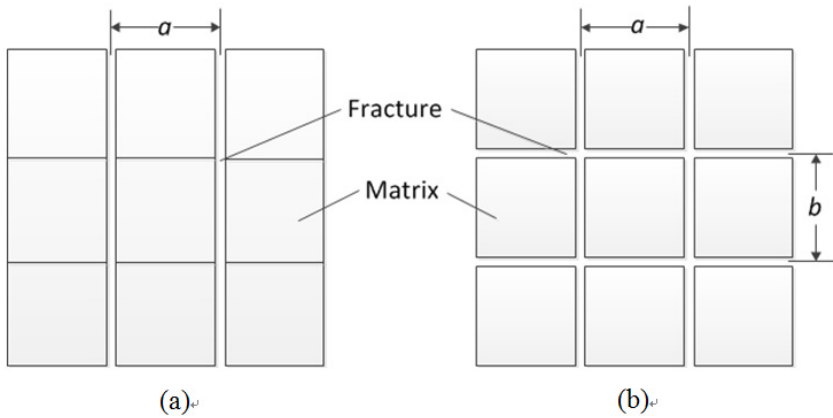


Figure 3: Idealized 1-D (a) and 2-D (b) fracture-matrix system.

### 2.2.3 Calculation of upscaled permeability tensor of active-fracture continuum

Many upscaling methods have been used to link the local scale to coarse support scale due to limitations of computer power [Luan, Sun, and Gu (2011); Gu, Zhang,

Yuan, and Ning (2012); Li, Wang, and Lee (2012)]. In this study, the fracture-matrix system is transformed into a grid-based continuum model (Fig.2 (b)), and the upscaled permeability tensor of each coarse block can be estimated by a DFN flow analysis for the underlying fracture network [Jackson, Hoch and Todman (2000); Pouya and Fouché (2009)]. In the present study, we used the method of Pouya and Fouché (2009) to calculate the equivalent permeability tensor of each coarse block which contains active fractures. Pouya and Fouché (2009) give a rigorous definition of the equivalent permeability tensor  $\mathbf{K}$  which relates mean flux  $\vec{Q}$  and the mean pressure gradient  $\vec{G}$  by an equation of the type

$$\vec{Q} = -\mathbf{K} \cdot \vec{G} \tag{7}$$

The permeability tensor  $\mathbf{K}$  is demonstrated to be symmetric and positive-definite under linear pressure boundary condition. The condition of linear pressure at the block contour (as shown in Fig.4) is defined by

$$p(\vec{x}) = \vec{A} \cdot \vec{x} + p, \tag{8}$$

where  $\vec{A}$  is a constant vector and  $p$  a constant scalar,  $\vec{x}$  is the position vector at block boundary.

The mean pressure gradient ( $\vec{G}$ ) is derived to be equal to the constant vector ( $\vec{A}$ ), and can be formulated as

$$\vec{G} = \vec{A} \tag{9}$$

For this case of a 2-D fracture system, mean flux is calculated by

$$\vec{Q} = \frac{1}{V} \sum_k f^{(k)} \vec{x}^{(k)}, \tag{10}$$

where  $V$  is the volume of the block,  $\vec{x}^{(k)}$  is the position vector of an intersection point of a fracture trace with the contour of the domain, and  $f^{(k)}$  is the flux going out of the trace at this point (Fig.4).

Consequently, the equivalent permeability tensor can be constructed by performing DFN flow simulations for two distinct directions (Fig.4) under linear pressure boundary conditions.

The inactive fracture-continuum and matrix continua contribute little to the global fluid flow, and are assigned relatively small permeability.

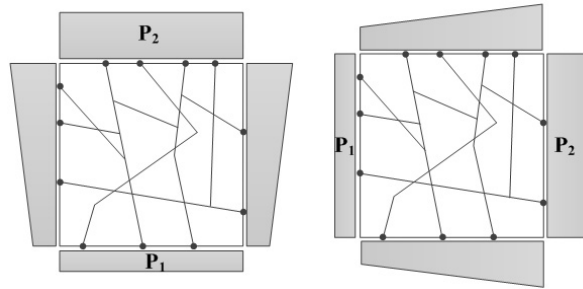


Figure 4: A representative block containing active fractures under linear pressure boundary condition in two distinct directions.  $P_2$ ,  $P_1$  is the constant hydraulic pressure at upstream and downstream boundary respectively.

### 3 Numerical examples

#### 3.1 Comparison with analytical solution

In this section, the multi-continuum model is applied to a wellbore flow problem extracted from Wu, Liu and Bodvarsson (2004). The problem under consideration is one-dimensional radial flow into a fully penetrating well in a radially infinite, horizontal reservoir that contains a set of uniform fractures (including active and inactive fracture) and matrix properties. Without consideration of wellbore storage and skin effects, Liu, Bodvarsson and Wu (2003) and Wu, Liu and Bodvarsson (2004) present an analytical solution of dimensionless pressure drop at the wellbore with a triple-porosity model. The basic parameters for the analytical solution and the derived model parameters for the multi-continuum model are listed in Tab. 2. The derived model parameters such as fracture spacing (matrix block size) and characteristic length of inactive fractures are determined from the given interporosity flow shape factor  $\alpha$  by using the Warren-Root pseudo-steady state model [Warren and Root (1963)].

Fig.5 shows the evolution of the pressure drawdown at the wellbore with comparison between numerical and analytical solutions. The pressure drawdown curve of the multi-continuum model with three continua (one active-fracture continuum, one inactive-fracture continuum and one matrix continuum, circles) shows good agreement with the analytical solution of the triple-porosity model (solid line), and exhibits three distinct, straight, parallel lines in semi-log space which corresponds to the effect of active, inactive fractures and matrix on fluid flow. The multi-continuum model with ten continua (two fracture continua and eight matrix continua, dashed line) shows a smoother pressure drop at intermediate time stage

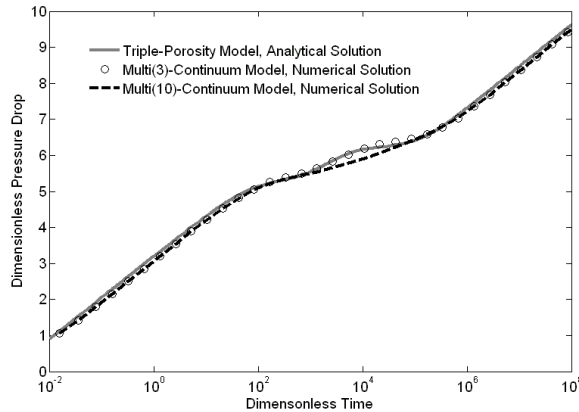


Figure 5: Comparison of pressure drawdown curves between numerical and analytical solutions

mainly due to that sub-gridding matrix block into more matrix continua can capture fully transient fracture-matrix interaction, while the triple-continuum model is limited to a quasi-steady state inter-porosity flow.

### 3.2 Application to a 2-D benchmark test (BMT) of DECOVALEX 2011

To study the effect of inactive fractures on the solute transport, we apply the multi-continuum model to a 2-D discrete fracture network, which is a benchmark test (BMT) of the DECOVALEX 2011 [Rutqvist, Leung, Hoch, Wang and Wang (2013)]. This BMT consists of a  $20 \times 20$  m model domain with a 2-D fracture-network model of 7797 individual fractures with fracture apertures correlated with fracture length (Fig.6). The model domain under low hydraulic pressure gradient of 10 Pa/m in horizontal direction is investigated. In our model simulations, we used a standard solute transport model which is part of the TOUGH2 code and applied the TOUGH2/EOS1 equation of state module [Pruess, Oldenburg and Moridis (1999)]. Water component 2 is injected at the inlet boundary in a pulse over a short time period, and then the mass flow of water component 2 at each outlet boundary is monitored to calculate breakthrough curves (BTC).

The study domain is discretized into  $40 \times 40$  blocks with overlapping sub-continua in each block based on the partitioning technique in Section 2. A heterogeneous, anisotropic permeability tensor field will be established finally in the study domain. The inactive fracture continuum and matrix continuum is assigned with a low permeability coefficient of  $1.0 \times 10^{-20}$  m<sup>2</sup> because of their insignificant contribution

Table 2: Parameters used in the wellbore flow problem using either a triple-porosity model or a multi-continuum model of the fractured reservoir

	Parameter	Value	Unit
Basic parameters	Matrix porosity	$\phi_M = 0.263$	
	Active fracture porosity	$\phi_F = 0.001$	
	Inactive fracture porosity	$\phi_f = 0.01$	
	Matrix permeability	$k_M = 1.572 \times 10^{-16}$	m <sup>2</sup>
	Active fracture permeability	$k_F = 1.383 \times 10^{-12}$	m <sup>2</sup>
	Inactive fracture permeability	$k_f = 1.383 \times 10^{-14}$	m <sup>2</sup>
	Total compressibility of three media	$C_M = C_F = C_f = 1.0 \times 10^{-9}$	1/Pa
	Well radius	$r_w = 0.1$	m
	Well production rate	$q = 100$	m <sup>3</sup> /day
	Formation thickness	$h = 20$	m
	F-M shape factor	$\alpha_{F-M} = 0.480$	m <sup>-2</sup>
	F-f shape factor	$\alpha_{F-f} = 0.351$	m <sup>-2</sup>
	f-M shape factor	$\alpha_{f-M} = 4.688$	m <sup>-2</sup>
	Water density	$\rho = 1000$	kg/m <sup>3</sup>
Water phase viscosity	$\mu = 1 \times 10^{-3}$	Pa·s	
Derived model parameters	Fracture spacing	$FS = 1.5$	m
	$f$ characteristic length	$l_f = 0.24$	m

to global fluid flow. The matrix porosity of each block is around 0.316% (considering isolated fractures in the block), and the matrix tortuosity is  $1.0 \times 10^{-2}$ . The molecular diffusion coefficient is  $1.0 \times 10^{-9}$  m<sup>2</sup>/s.

The BTC at the three flow outlet boundaries is compared for simulation results derived by different research teams in the DECOVALEX project using different models (Fig.7). The IC team used the NAPSAC DFN model and particle tracking method for simulating solute transport; KTH team used distinct element method with UDEC and particle tracking method [Rutqvist, Leung, Hoch, Wang and Wang (2013)]. The BTCs obtained by the above three models show a reasonably good agreement and exhibit long tailing behavior of solute transport under low hydraulic pressure gradient due to rock matrix diffusion.

The effect of inactive fractures on solute transport is investigated through a comparison of solute concentration evolution in the rock matrix (Fig. 8a) and breakthrough curves (Fig. 8b) between multi-continuum model and active-fracture model. In the active-fracture model we did not consider the effect of inactive fractures, but we used the same permeability tensor field, determined from DFN flow simulations in the local coarse block. The comparison of the results in Fig. 8 indicates that the inactive fractures enhance rock matrix diffusion via increasing contact areas be-

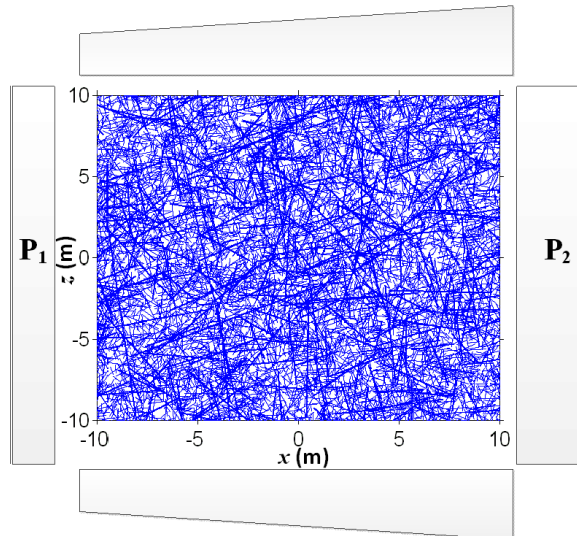


Figure 6: A 20×20 m 2-D fracture network model with 7797 fractures under horizontal hydraulic pressure gradient

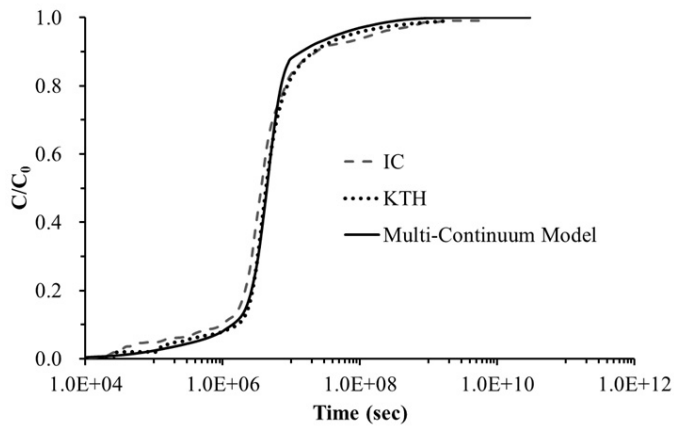


Figure 7: Comparison of breakthrough curves among different research teams

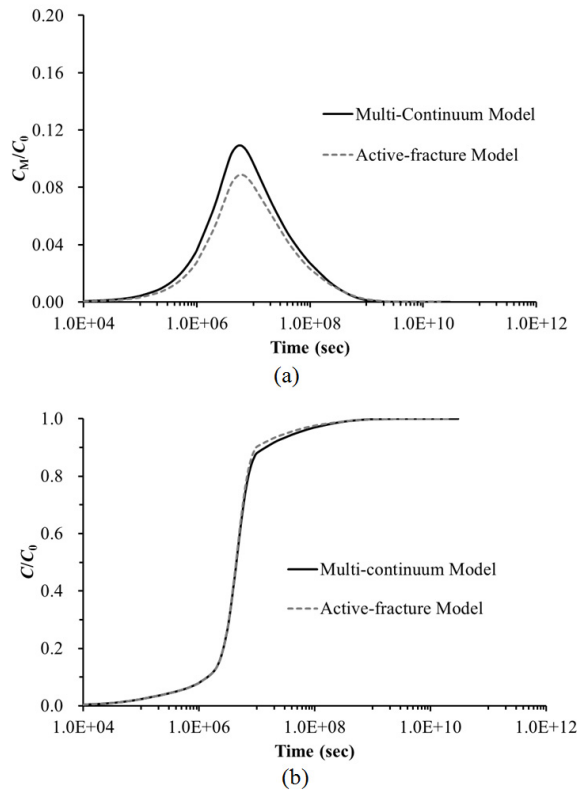


Figure 8: A comparison between the multi-continuum model and the active-fracture model: (a) evolution of solute concentration in the rock matrix; (b) Breakthrough curves.

tween fracture and matrix systems (Fig. 8a) and impact the overall solute transport behavior (Fig. 8b). The enhancement of rock matrix diffusion in this case is not very strong due to the fact that this is a very dense and well-connected fracture network in which the total volume fraction of inactive fractures ( $0.18 \times 10^{-3}$ ) is one order of magnitude less than that of active fractures ( $0.11 \times 10^{-2}$ ). However, we can still infer that although inactive fractures do not significantly impact the total flow through the model, it can have a significant impact on the solute transport.

#### 4 Conclusions

In this paper a multi-continuum model which can consider the effect of inactive fractures was developed. The model was verified against an analytical solution of a wellbore flow problem, and then applied to a 2-D fracture network system to study

the effect of inactive fractures on solute transport. The simulation indicates that the inactive fractures, which although have little contribution to global fluid flow, will increase the contact areas between fracture and matrix systems, and this will enhance rock matrix diffusion and impact the overall transport behavior. This enhancement of matrix diffusion through inactive fractures in a 2-D fracture network is also consistent with the findings of field scale experiments [Zhou, Liu, Bodvarsson and Molz (2006)].

### **Acknowledgements**

Financial support from the National Basic Research Program of China (973 Program: 2011CB013800) and by the U.S. Department of Energy under contract No. DE-AC02-05CH11231 is greatly appreciated.

### **References**

- An, Y. S.; Wu, X. D.; Gao, D.L.** (2012): On the Use of PEBI Grids in the Numerical Simulations of Two-Phase Flows in Fractured Horizontal Wells. *CMES-Computer Modeling in Engineering & Sciences*, vol. 89, no. 2, pp. 123-141.
- Baghbanan, A.; Jing, L. R.** (2007): Hydraulic properties of fractured rock masses with correlated fracture length and aperture. *International Journal of Rock Mechanics and Mining Sciences*, vol. 44, no. 5, pp. 704-719.
- Barenblatt, G. I.; Zheltov, I. P.; Kochina, I. N.** (1960): Basic concepts in the theory of seepage of homogeneous liquids in fissured rocks [strata]. *Journal of Applied Mathematics and Mechanics*, vol. 24, no. 5, pp. 1286–1303.
- Dershowitz, B.; LaPointe, P.; Eiben, T.; Wei, L. L.** (2000): Integration of discrete feature network methods with conventional simulator approaches. *Spe Reservoir Evaluation & Engineering*, vol. 3, no. 2, pp. 165-170.
- Dogan, M. O.; Class, H.; Helmig, R.** (2009): Different concepts for the coupling of porous-media flow with lower-dimensional pipe flow. *CMES-Computer Modeling in Engineering & Sciences*, vol.53, no. 3, pp. 207-233.
- Doughty, C.** (1999): Investigation of conceptual and numerical approaches for evaluating moisture, gas, chemical, and heat transport in fractured unsaturated rock. *Journal of Contaminant Hydrology*, vol. 38, pp. 69-106.
- Doughty, C.; Salve, R.; Wang, J. S. Y.** (2002). Liquid-release tests in unsaturated fractured welded tuffs: II. Numerical modeling. *Journal of Hydrology*, vol. 256, pp. 80-105.
- Gato, C.; Shie, Y.** (2008): Numerical Simulations of Dynamic Fracture in Thin Shell Structures. *CMES-Computer Modeling in Engineering & Sciences*, vol. 33,

no. 3, pp. 269-292.

**Gu, B.; Zhang, L. C.; Yuan, W.F.; Ning, Y. J.** (2012): A Multi-Scale Computational Method Integrating Finite Element Method with Atomic Interactions of Materials. *CMES-Computer Modeling in Engineering & Sciences*, vol. 88, no. 4, pp. 309-324.

**Jackson, C. P.; Hoch, A. R.; Todman, S.** (2000): Self-consistency of a heterogeneous continuum porous medium representation of a fractured medium. *Water Resources Research*, vol. 36, no. 1, pp. 189-202.

**Karimi-Fard, M.; Gong, B.; Durlafsky, L. J.** (2006): Generation of coarse-scale continuum flow models from detailed fracture characterizations. *Water Resources Research*, vol. 42, no. 10, pp. W10423.

**Li, J. Y.; Wang, X. Q.; Lee, J. D.** (2012): Multiple Time Scale Algorithm for Multiscale Material Modeling. *CMES-Computer Modeling in Engineering & Sciences*, vol. 85, no. 5, pp. 463-480.

**Liu, J.; Bodvarsson, G. S.; Wu, Y.** (2003): Analysis of flow behavior in fractured lithophysal reservoirs. *Journal of Contaminant Hydrology*, vol. 62-63, pp. 189-211.

**Long, J. C. S.; Remer, J. S.; Wilson, C. R.; Witherspoon, P. A.** (1982): Porous media equivalents for networks of discontinuous fractures. *Water Resources Research*, vol. 18, no.3, pp. 645-658.

**Luan, K.; Sun, B. Z.; Gu, B. H.** (2011): A Multi-scale Geometrical Model for Finite Element Analyses of Three-dimensional Angle-Interlock Woven Composite under Ballistic Penetration. *CMES-Computer Modeling in Engineering & Sciences*, vol. 79, no. 1, pp. 31-61.

**Min, K. B.; Jing, L.; Stephansson, O.** (2004): Determining the equivalent permeability tensor for fractured rock masses using a stochastic REV approach: Method and application to the field data from Sellafield, UK. *Hydrogeology Journal*, vol. 12, no. 5, pp. 497-510.

**Neretnieks, I.** (2002): A stochastic multi-channel model for solute transport - analysis of tracer tests in fractured rock. *Journal of Contaminant Hydrology*, vol. 55, pp. 175-211.

**Oda, M.** (1985): Permeability Tensor for Discontinuous Rock Masses. *Geotechnique*, vol. 35, no. 4, pp. 483-495.

**Pouya, A.; Fouché, O.** (2009): Permeability of 3D discontinuity networks: New tensors from boundary-conditioned homogenisation. *Advances in Water Resources*, vol. 32, no. 3, pp. 303-314.

**Pruess, K.** (1983): GMINC- A mesh generator for flow simulations in fractured

reservoirs, *Tech. Rep. LBNL-15227 Lawrence Berkeley National Laboratory*.

**Pruess, K.; Karasaki, K.** (1982): Proximity function for modeling fluid and heat flow in reservoirs with stochastic fracture distributions. *The eighth workshop on geothermal reservoir engineering Stanford University, Stanford CA*.

**Pruess, K.; Narasimhan, T. N.** (1982): A Practical Method for Modeling Fluid and Heat-Flow in Fractured Porous-Media. *Society of Petroleum Engineers Journal*, vol. 25, no. 1, pp. 14-26.

**Pruess, K.; Oldenburg, C.M.; Moridis, G.J.** (1999): TOUGH2 User's Guide Version 2. *Tech. Rep. LBNL-43134, Lawrence Berkeley National Laboratory*.

**Rutqvist, J.; Leung, C.; Hoch, A.; Wang, Y.; Wang, Z.** (2013): Linked multi-continuum and crack tensor approach for modeling of coupled geomechanics, fluid flow and transport in fractured rock. *Journal of Rock Mechanics and Geotechnical Engineering* vol. 5, no. 1, pp. 18-31.

**Smith, G. E.; Crocker, A. G.; Flewitt, P. E. J.; Mahalingam, S.** (2012): Creating Three-Dimensional Models to Investigate Brittle Fracture in Polycrystalline Metals. *CMC-Computers Materials and Continua*, vol. 31, no. 1, pp. 17-36.

**Tatomir, A. B.; Szymkiewicz, A.; Class, H.; Helmig, R.** (2011): Modeling Two Phase Flow in Large Scale Fractured Porous Media with an Extended Multiple Interacting Continua Method. *CMES-Computer Modeling in Engineering & Sciences*, vol. 77, no. 2, pp. 81-112.

**Warren, J.; Root, P.** (1963): The behaviour of naturally fractured reservoirs. *Society of Petroleum Engineers*, vol. 228, pp. 245-255.

**Wu, Y.; Liu, H. H.; Bodvarsson, G. S.** (2004): A triple-continuum approach for modeling flow and transport processes in fractured rock. *Journal of Contaminant Hydrology*, vol. 73, pp. 145-179.

**Xu, C.; Dowd, P.; Mardia, K.; Fowell, R.** (2006): A Connectivity Index for Discrete Fracture Networks. *Mathematical Geology* vol. 38, no. 5, pp. 611-634.

**Zhao, Z.; Jing, L.; Neretnieks, I.; Moreno, L.** (2011): Numerical modeling of stress effects on solute transport in fractured rocks. *Computers and Geotechnics*, vol. 38, no. 2, pp. 113-126.

**Zhou, Q.; Liu, H. H.; Bodvarsson, G. S.; Molz, F. J.** (2006): Evidence of multi-process matrix diffusion in a single fracture from a field tracer test. *Transport in Porous Media*, vol. 63, no. 3, pp. 473-487.

**Zhou, Q.; Liu, H. H.; Molz, F. J.; Zhang, Y.; Bodvarsson, G.S.** (2007): Field-scale effective matrix diffusion coefficient for fractured rock: Results from literature survey. *Journal of Contaminant Hydrology*, vol. 93, pp. 161-187.

**Zuo J. P.; Peng S. P.; Li Y. J.; Chen Z. H.; Xie H. P.** (2009): Investigation of

karst collapse based on 3-D seismic technique and DDA method at Xieqiao coal mine, China. *International Journal of Coal geology*, vol. 78, no. 4, pp. 276-287.

**Zuo, J. P.; Xie, H. P.; Zhou H. W.; Peng S. P** (2010): SEM in-situ investigation on thermal cracking behavior of Pingdingshan sandstone at elevated temperatures. *Geophysical Journal International*, vol. 181, no. 2, pp. 593-603.